Structure Investigations on Drawn High-Density Blown PE Films

D. HOFMANN, D. GEISS, and A. JANKE, *Academy of Sciences of the German Democratic Republic, Institute of Polymer Chemistry "Erich Correns", Teltow-Seehof, GDR-1530, German Democratic Republic*, G. H. MICHLER, *Institute of Solid State Physics and Electron Microscopy, Halle / S., GDR-4050, German Democratic Republic,* and P. FIEDLER, *VEB Leuna-Werke "Walter Ulbricht," Leuna, German Democratic Republic*

Synopsis

The supermolecular structure of blown HDPE films, which were obtained by a combination of film blowing under a very low blowup ratio and slow takeoff velocity with subsequent uniaxial drawing, is characterized using WAXS texture and profile analysis, EM and mechanical investigations. Samples with low uniaxial drawing ratios ($\lambda \lesssim 1.5$) contain low stress crystalline and transcrystalline material and show an a-texture, while samples with higher uniaxial drawing ratios only consist of high stress crystalline material and show a c-texture. With one exception the results of texture investigations can be related to the results of the mechanical investigations.

INTRODUCTION

Blown polyethylene (PE) film is one of the most important polymeric mass products. For this reason, already, therefore, structure investigations of this material are of high scientific interest. The film blowing process is characterized by a very complex structure formation caused by different parallel crystallization and orientation processes. Widely used parameters for the characterization of the blowing process are the temperature T_m, the viscosity of the melt, the axial (i.e., parallel to the machine direction M of the film) and lateral [i.e., parallel to the plane formed by the transverse (T) and normal (N) directions of the film] blowing stress components σ_{11} and $\sigma_{22} = \sigma_{33}$, respectively. The drawing ratio λ (amount of axial stretching of the extruded melt), the blowup ratio β (ratio of film-tube diameter at the freeze line to the extrusion die diameter), the thickness of the blown foil, the freeze line height, and the axial take-off velocity V_A at the height of the niprollers, which transport the film tube upward, additionally forming an air-tight seal of the bubble (see also below).

The material properties of the final blown PE films may vary with varying processing parameters. In this connection structure investigations are often carried out with the aim of revealing correlations between the processing parameters, the determined structural parameters, and the macroscopic mechanical properties, which is very difficult because of the complex nature of the structure formation during the film blowing process. Good correlations were often found between some mechanical parameters of the foil and the

Journal of Applied Polymer Science, Vol. 39, 1595–1611 (1990)
 CCC 0021-8995/90/071595-17$04.00

state of orientation of the crystalline molecular chain axes (c-axes) at the surface (M, T-plane) of the sample.[1-3] The interest in texture investigations of tubular PE foils, which began in the fifties, mainly resulted from these correlations.

At the beginning only flat plane X-ray cameras were used for obtaining some texture data.[4-7] Lindenmeyer and Lustig[1] first prepared WAXS-pole figures for the characterization of a-, b-, and c-axes orientation for LDPE and HDPE blown films. Furthermore, they pointed out the fundamental limitations of WAXS-flat film techniques in the field of texture characterization. Desper[2] investigated PE films which were produced under varying deformation stresses during the blowing process. Pole figures were shown from which biaxial orientation factors (cf. Ref. 8) were determined and discussed. Samples obtained under a small blowup pressure and slowly cooled in the freezing zone showed a preferential orientation of a-axes in the M- and b-axes in the N-direction. Contrarily, high blowup pressure and fast freezing resulted in films with a uniaxial orientation with the a-axes in the M direction as in the former case but with b- and c-axes isotropically oriented in the N–T plane.

Maddams and Preedy[1,9-11] published results of very extensive texture investigations for very different blown HDPE films (T_m = 455–523 K, λ = 1.1–6.0, β = 0.5–7). A comparison between orientation factors for the c-axes concerning the sample directions M, N, T and some mechanical properties of the films did not reveal any correlation. This fact was interpreted as being due to the very complex texture of the samples. Therefore, Maddams and Preedy restricted their discussion to the visual interpretation of (200)-, (110)-, (020)-, and in some cases also of the (011)-pole figures. Nearly all samples investigated showed very much scattering in the orientation of lattice planes normals. Additionally there were some maxima of orientation for the crystallographic a-, b-, and c-axes, which could be mainly connected with the stress crystallization types discussed below.

For one sample, however, Maddams and Preedy found, besides a preferential stress crystallization type b-axes orientation in T, also an additional orientation maximum of b-axes in the N-direction connected with a transcrystalline portion of material (cf. also below). But they were not able to correlate this finding with the special preparation conditions. The results of Maddams and Preedy concerning stress crystallization under intermediate stresses were confirmed by publications of Matsumata and Nagasawa,[12] Shimomura et al.,[13] and Gilbert et al.[14]

Choi et al.[15] mainly investigated the connection between the axial and lateral stress components acting on the PE melt bubble at freeze line and the resulting texture of the final film. For samples without any blowup pressure (i.e., $\sigma_{22} = 0$) and with only a small axial stress σ_{11}, a preferential orientation of a-axes in M and an isotropic orientation of b-axes in the N–T plane were revealed. For $\sigma_{22} = 0$ and a high σ_{11}-value the b-axes remained in the N–T plane but with a slight concentration in the T-direction, while the a-axes were preferentially oriented along a small circle with an angle of approximately 60° to the M-direction.

For a film with σ_{11}/σ_{22} ratio of 4:1 the b-axes again remained perpendicular to the M-direction, but now with a slight concentration towards the film normal N. The a-axes showed nearly the same behavior as in the former case,

but now with slight orientation maxima in the pole figure in the region of the points of intersection of the mentioned small circle with the great circle across M and N. For a σ_{11}/σ_{22} ratio of 1:1.5 the b-axes showed a distinct orientation in normal direction, while the a- and c-axes were isotropically distributed in the surface of the film. Thus, Choi et al.[15] in most cases found more complicated textures as Maddams and Preedy,[3,9] who mostly got relatively simple uniplanar-axial textures for the materials investigated by them.

Otherwise, we have previously reported texture investigations on blown LDPE films.[16] The studied materials were industrial products with only slight variations in the processing parameter. For most of the samples we found a uniplanar-axial texture with the a-axes concentrated in M- and the b-axes in

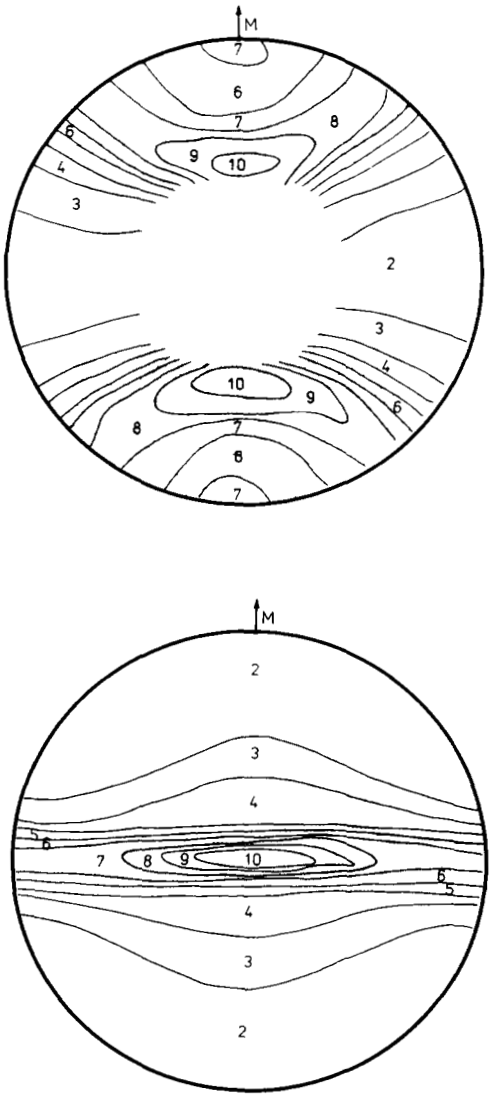

Fig. 1. Pole figures of a blown LDPE-film after Walenta et al.[16]: $\beta = 2$, $V_A = 40$ m/min; (a) (200) transmission mode pole figure; (b) complete (020) pole figure.

N-directions (a-texture). This type of orientation was also observed by-Desper[2] for some blown PE samples. But for a sample with a high take-off velocity (V_A = 40 m/min instead of 14 m/min) in comparison to the other samples, we found a texture comparable to that described by Choi et al.[15] for the sample with σ_{11}/σ_{22} = 4:1 ratio (cf. Fig. 1).

In the paper cited[14] these results were related to the occurrence of monoclinic crystallites besides the main fraction of orthorhombically crystalline material. But, taking into consideration the results of our recent investigations of blown HDPE films, which will be reported in the following sections, we will critically reinterpret the yields cited above.

For the investigations we shall present here, preparation conditions were chosen such that in each case mainly one single processing parameter was dominating the blowing process. In the first series of investigations reported here the take-off velocity V_A, the blowup ratio β, and the draw ratio λ were minimized and the films blown in such a manner were uniaxially drawn after solidification. Thus it was possible to simulate both a blowing process under very low stresses and a blowing process with very high axial stresses (σ_{11}).

The main aim of these studies was the characterization of the influence of the different crystallization mechanisms on the formation of the samples textures and supermolecular structures. It should be noted that besides WAXS-pole figures some orientation-dependent crystallite sizes and some mechanical parameters were used for the discussion.

EXPERIMENTAL

Preparation of Samples

A HDPE of type A62 ($M_w \approx 10^5$) made by VEB Chemische Werke Buna (G.D.R.) was used as the starting product for the film blowing process. Sample 1 was blown in a commercial film blowing unit with a very small drawing ratio ($\lambda \approx 1$, V_A = 1.2 m/min) and blowup ratio ($\beta \approx 1$). This sample then was uniaxially drawn in the M-direction at room temperature with λ = 1.1 (sample 2), λ = 5.0 (sample 3), and λ = 7.5 (sample 4), respectively.

WAXS Measurements

Transmission pole figures and, where necessary, also complete pole figures were prepared by the WAXS technique described in Ref. 17 for the (200)- and (020)-lattice planes of each sample, for the (011)-lattice planes of samples 1 and 2, and for the (002)-lattice planes of samples 3 and 4. Representative examples of the respective pole figures are shown in Figures 2–6.

Furthermore, for the samples 1, 2, and 4 the WAXS intensity $I(2\nu)$ of the (110)-, (200)- and (020)-reflection of the orthorhombic PE modification was measured using a horizontal X-ray counter diffractometer HZG-4A (VEB Freiberger Präzisionsmechanik) with Ni-filtered CuK_α-radiation in symmetrical transmission as well as in symmetrical reflection modes in order to get crystallite size parameters for differently oriented portions of crystalline material. In this connection the samples 1 and 2 were fixed in the sample holder in such a manner that in transmission mode the registration of WAXS took place for all crystallites with the respective scattering lattice plane

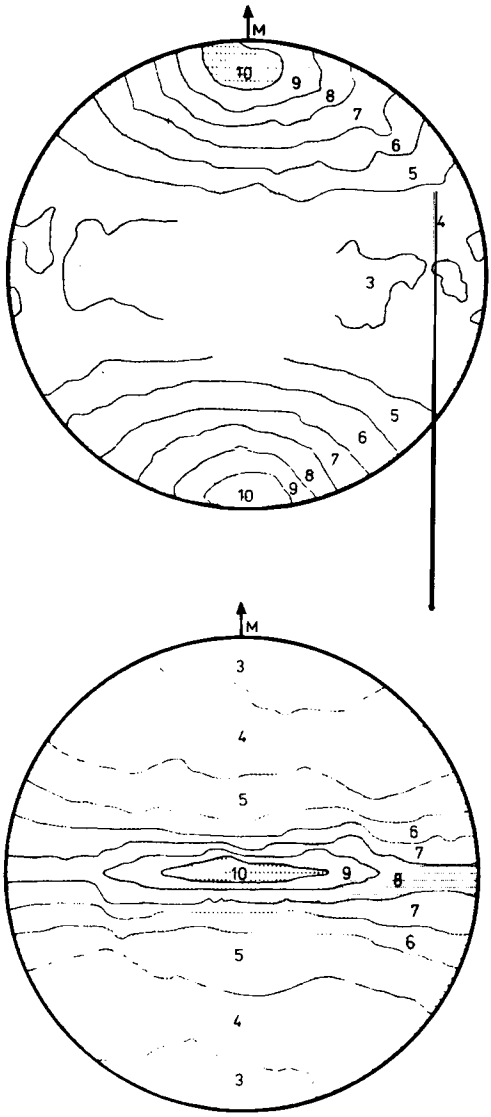

Fig. 2. Pole figures of sample 1: (a) (200) transmission mode pole figure; (b) (020) complete pole figure.

normals oriented in the M-direction of samples. In connection with the qualitative and quantitative changes in texture, the WAXS of the (110) and (200) peak, respectively, was only measured in reflection mode in the case of sample 4, while the registration of the (020) peak of sample 4 was performed in symmetrical transmission mode for all crystallites with their b-axes in the transverse direction T of the film.

In the reflection case for all samples the WAXS of the crystallites with their respective lattice plane normals directed towards N was obtained. Owing to the very pronounced scattering of the c-axes orientation distribution, a quantitatively evaluable WAXS profile of the (002) reflection was not

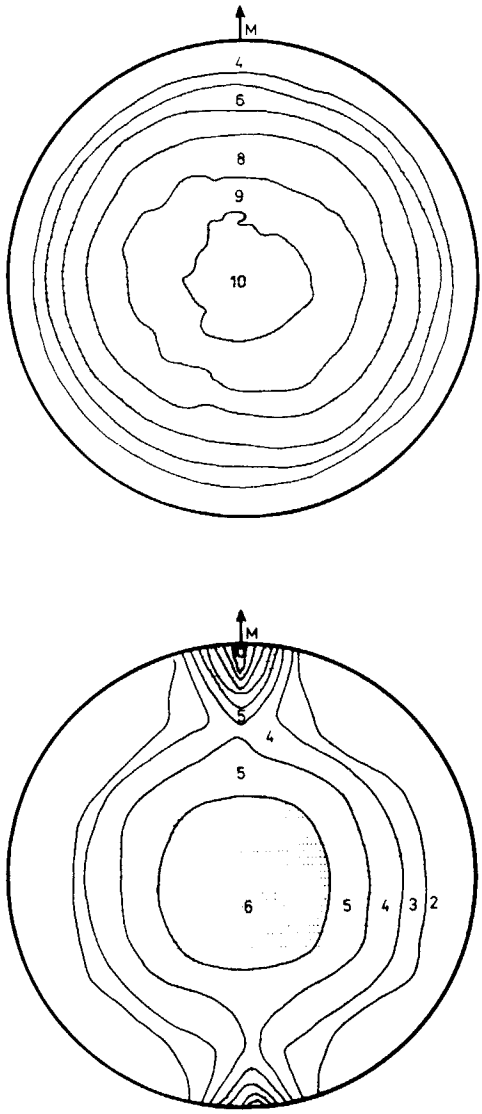

Fig. 3. Pole figures of samples 1 and 4: (a) (011) complete pole figure of sample 1; (b) (002) complete pole figure of sample 4.

obtained in the case of samples 1 and 2. But this was possible for sample 4, for which the WAXS of the (002) reflection was obtained in symmetrical transmission mode for the crystallites with their c-axes oriented in the M-direction.

The WAXS-intensities $I(2\nu)$ gained were corrected for parasitic scattering, absorption, polarization, $CuK_{\alpha_1\alpha_2}$ doublet broadening (cf. Ref. 18), and background scattering. Necessary resolution of overlapping reflections was performed via a Pearson-VII-function fit program.[19,20]

From these corrected scattering curves, minimum mean crystallite size parameters $L_{hkl,N}$, $L_{hkl,M}$, and $L_{hkl,T}$ (N = normal direction, M = machine direction, and T = transverse direction of the sample) were calculated from

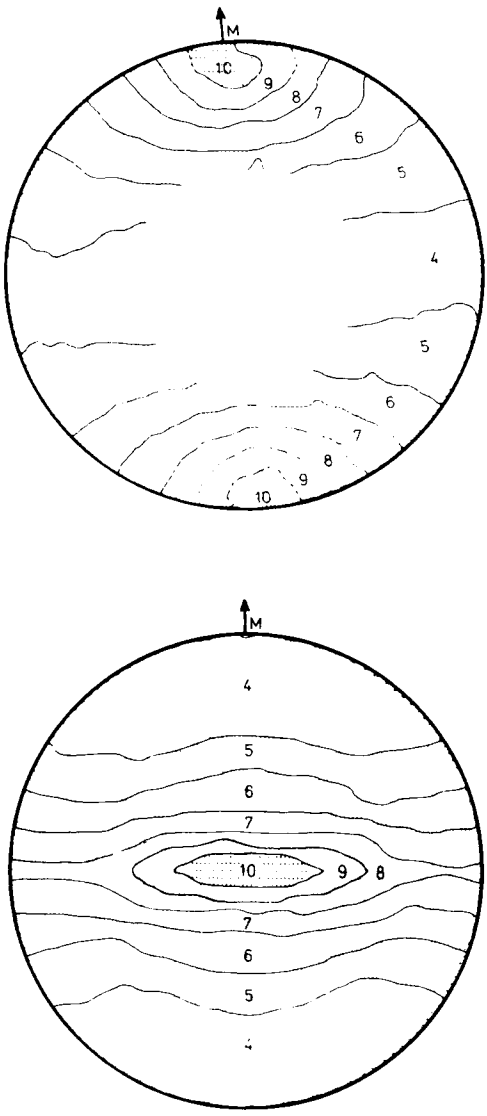

Fig. 4. Pole figures of sample 2: (a) (200) transmission mode pole figure; (b) (020) complete pole figure.

the full half-width b of the respective reflection using the Scherrer equation

$$L_{hkl} = (0.89 \cdot \lambda)/(b \cos \nu_{max})$$

with ν_{max} being the scattering angle at maximum intensity of the respective reflection and λ the wavelength of the X-rays used. All quantitative results are shown in Table I.

Mechanical Investigations

For all samples the stress–strain curves were recorded quasistatically at 296 K using an Instron tensile tester. Young's modulus was then calculated from

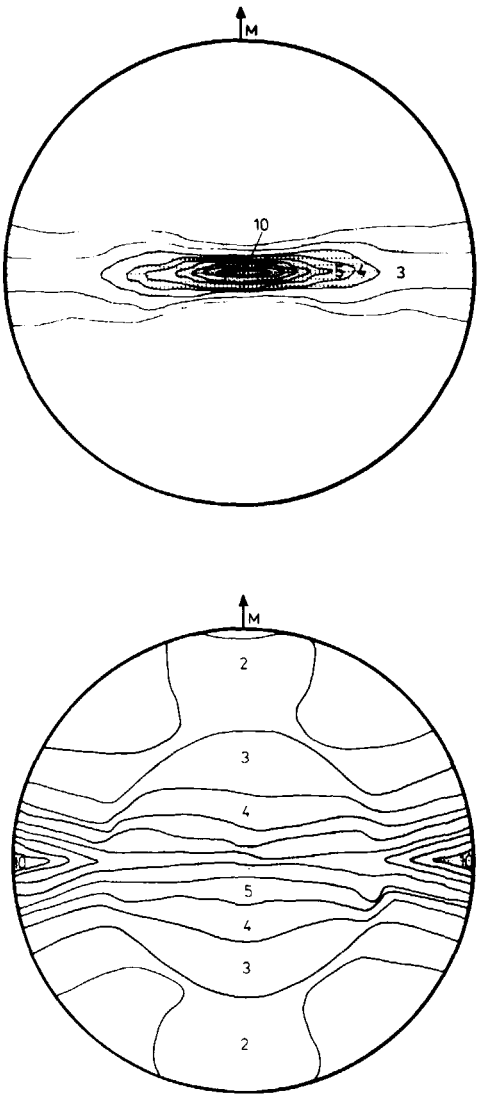

Fig. 5. Pole figures of sample 3: (a) (200) complete pole figure; (b) (020) complete pole figure.

these curves. Additionally respective tensile strength values and elongations at break have been determined.

RESULTS AND DISCUSSION

Here at first it seems to be useful to give a short summary about the PE film blowing process and about models for the description of the different types of crystallites, which may be present in PE-blown films.

The properties of the melt used in the blowing process are essentially determined by melt temperature T_m and melt viscosity. The melt is extruded through an annular die and afterwards drawn upwards in machine direction (M) by making use of a take-off mechanism. Air is blown into the molten film

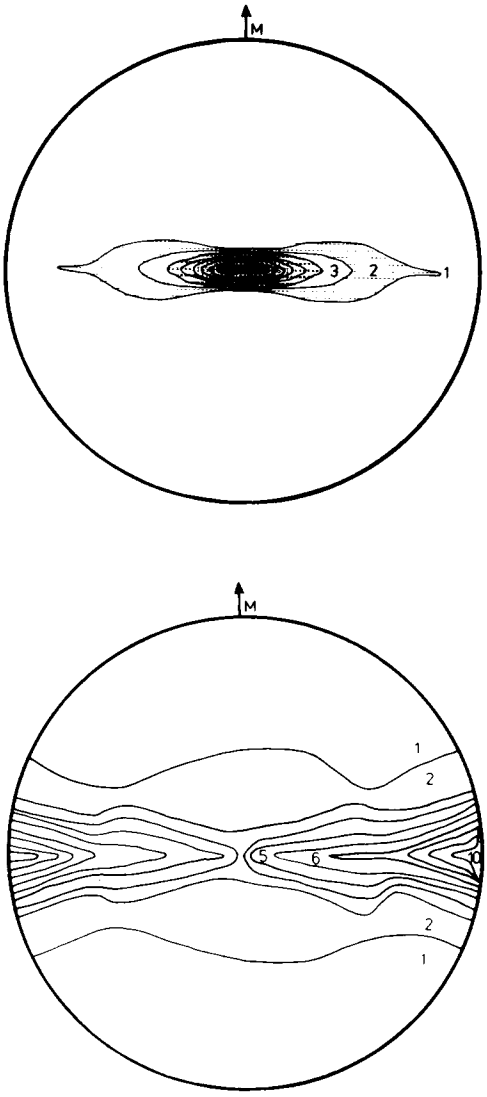

Fig. 6. Pole figures of sample 4: (a) (200) reflection mode pole figure; (b) (020) complete pole figure.

tube for inflating the tube and forming a bubble. During this process there are axial stresses in machine direction and lateral stresses in transverse (T)-, and normal (N)-directions resulting from the melt, extrusion, take-off, and blowup conditions. These stresses will cause some orientation of the molecular chain axes in the melt. Contrary to that, there are also orientation relaxation processes during the film blowing. These processes may mainly depend on the solidification time of the melt in the freezing zone, the melt temperature T_m, and the melt viscosity. The solidification in its part is accompanied by a partial crystallization. Because of this complicated situation it is necessary to use specific models for the combined crystallization and orientation processes in order to interpret the results of structure investigations.

TABLE I
Quantitative Results of the WAXS Investigations[a]

Parameter	Sample 1	Sample 2	Sample 3	Sample 4
ΔB^{200}_{N-M}	22	22	2	< 2
ΔB^{200}_{N-T}	—	—	26	18
ΔB^{020}_{N-M}	10	16	2	2
ΔB^{020}_{N-T}	74	68	16	13
$L_{200,M}$(nm)	9.9	9.7	—	—
$L_{200,N}$(nm)	19.4	18.7	—	8.4
$L_{200,T}$(nm)	—	—	—	7.3
$L_{110,M}$(nm)	9.9	10.1	—	—
$L_{110,N}$(nm)	25.8	28.7	—	9.1
$L_{110,T}$(nm)	—	—	—	8.4
$L_{020,M}$(nm)	10.4	10.4	—	—
$L_{020,N}$(nm)	14.4	11.8	—	7.0
$L_{020,T}$(nm)	—	—	—	8.7
$L_{002,M}$(nm)	—	—	—	9.3

[a] ΔB^{hkl}_{N-M} = range of the highest class of intensity of the (hkl)-pole figure in N–M direction. ΔB^{hkl}_{N-T} = range of the highest class of intensity of the (hkl)-pole figure in N–T direction. $L_{hkl,M}$ = weight average crystallite size perpendicular to the (hkl)-lattice planes for crystallites, for which the normals at their respective scattering lattice planes are directed in the M-direction. $L_{hkl,N}$ and $L_{hkl,T}$ are analogous to $L_{hkl,M}$.

The shear stresses acting on the melt during extrusion through the annular die and during the blowing and take-up stage of the process cause a partial chain extension. The extended chain sections are assumed to be nuclei for bulk crystallization taking place at and above the freeze line. This type of crystallization which is called "stress crystallization" was first described as the row orientation process by Keller et al.,[6,21,22] and further improved by Maddams and Preedy[3,9,10]: If the stresses during the bulk crystallization are very low, the so-called "low-stress" crystallization occurs, with the a-axis of crystallites preferentially oriented in the M-direction (a-texture), the b-axes (growth direction) aligned along the T-direction, and the c-axes mainly oriented in the direction of film normal N [cf. Fig. 7(a). Under intermediate deformation stresses the preferential orientation of the crystalline b-axes along the T remains, but the a-axes show a higher degree of orientation along the M–N great circle of the respective (200)-pole figure with the maximum at an angular distance of 20–50° to the M-direction.

Under relatively high deformation stresses (high stress crystallization) this angle increases to values of 60° and more. For very high stresses (e.g., via very high take-off velocities) a preferential orientation of crystalline a-axes in the N-direction and, therefore, of c-axes in the M-direction (c-texture) may be obtained, too[10] [cf. Fig. 7(b)].

While the stress crystallization types after Keller and Machin[21] are caused by nucleation in the volume, for blown PE films there exists also an additional possibility for a crystallization mechanism, the transcrystallization process,[3,23,24] in which case crystallization starts from the nuclei at the surface of the foil tube, mainly controlled by the freeze temperature gradient along the N-direction. This results in a preferential orientation of the crystallographic b-axes towards the film normal N. The a- and c-axes are isotropically oriented in the film surface [cf. Fig. 7(c)].

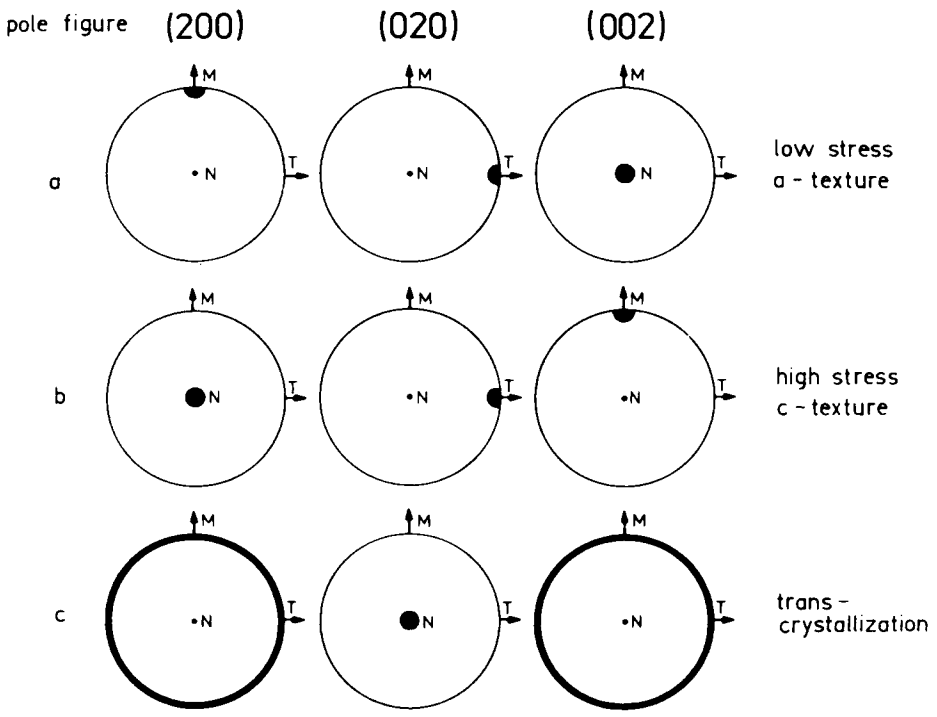

Fig. 7. Schematic representation of ideal states of orientation for different crystallization processes which may occur during PE-film blowing.

During the PE-foil blowing process, transcrystallization occurs in addition to stress crystallization. In this connection transcrystallization might be the dominant process, if T_m is much higher than crystallization temperature, if there is a great gradient of temperature in the freezing zone, and if the blown film is relatively thin.[9] Discussing the results of our structure investigations, it should be first mentioned that for the samples studied here only the orthorhombic crystalline modification of PE ($a = 0.740$ nm, $b = 0.493$ nm, $c = 0.534$ nm)[25] was detected.

Figures 2–6 exhibit the (200)-, (020)-, (011)-, and (002)-pole figures, respectively, for the HDPE blown films under consideration. (Note: For orthorhombic PE the angle between the (011)- and (002)-lattice plane normals is ~ 27°). The (011)-pole figure of sample 2 corresponds qualitatively to the respective pole figure of sample 1. In the same way the (002)-pole figures of the films 3 and 4 can be compared.

The nearly unstretched sample 1 possesses a texture of distinct diffusion [cf. Figs. 2 and 3(a)]. The crystalline a-axes are preferentially oriented along M, and the b-axes shown an orientation maximum in the N-direction. From the intensity distribution in the (011)-pole figure, however, one has to assume a c-axes orientation distribution with a slight maximum approximately also in the N-direction. The following interpretation of the pole figures shown, which is based on the crystallization models discussed above, seems to be reasonable:

In sample 1 both transcrystallization starting from the film surface and "low-stress" crystallization starting in the bulk occur. The first mentioned crystallization mechanism is connected with a preferential orientation of

b-axes in the N-direction, while the a- and c-axes are randomly distributed in the M–T plane [cf. Fig. 7(c)]. For the second crystallization type under very low stress conditions, however, the orientation maxima are for a-axes the M-direction, for b-axes the T-direction, and for c-axes the N-direction of the films [cf. Fig. 7(a)]. All these preferential orientations are usually connected with considerable diffusion,[3] which is first of all an explanation for the diffusion also observed for the practically measured pole figures of sample 1. With one exception the theoretical orientation maxima shown in Figures 7(a) and 7(c) are to be seen in the measured pole figures [cf. Figs. 2 and 3(a), respectively]. Therefore, we assume the orientation distribution measured for sample 1 to be a superposition of the orientation distribution of the transcrystalline and low stress crystallization type portions of material in the blown film just mentioned. (Note: The fact that a distinct maximum of orientation in T in the (020)-pole figure of sample 1 cannot be seen is probably connected with the fact that the maximum of intensity of the transcrystalline material around N will decrease only slowly in N–T-direction, which is also quantitatively established (cf. ΔB^{020}_{N-T} in Table I).

The results of crystallite size determination also confirm the assumption of two differently crystallized portions of material in sample 1 (cf. Table I). For crystallites with their a-axes directed along M, the crystallite size value $L_{200/M}$ was found to be 9.9 nm. Crystallites with their b-axes parallel to M have $L_{020,\,M} = 10.4$ nm, and crystallites with their (110)-lattice plane normals preferentially oriented in the M-direction have $L_{110,\,M} = 9.9$ nm, while the crystallite sizes are considerably greater for crystallites with their a-axes, b-axes and (110)-lattice plane normals, respectively, oriented in the N-direction:

$$L_{200,\,N} = 19.4 \text{ nm}, \qquad L_{020,\,N} = 14.4 \text{ nm}, \qquad L_{110,\,N} = 25.8 \text{ nm}$$

The crystallites contributing to the average crystallite sizes $L_{200,\,N}$, $L_{020,\,M}$, and $L_{110,\,M}$, respectively, are oriented in such a manner that the respective net plane normals are directed relatively far away from the respective ideal orientation maxima of the crystallization types. But crystallite sizes measured in symmetrical reflection mode (e.g., $L_{200,\,N}$) are very sensitive about the surface layer of the sample where the transcrystalline material portion is assumed to exist, while crystallite sizes like $L_{020,\,M}$ and $L_{110,\,M}$ are averages over the whole sample volume. Moreover, the average size parameter $L_{200,\,M}$ results from contributions of crystallites with crystalline a-axes oriented in the M-direction which is typical for "low-stress" crystallization. In the case of $L_{020,\,N}$, just those crystallites contribute which belong to the transcrystalline material portion. Finally the b-axes of the crystallites causing $L_{110,\,N}$ are oriented along a small circle with an angle of 33.7° to the N-direction of the film. But this is in the region of the (020)-pole figure where the transcrystalline material proportion has its orientation maximum.

Therefore, it is to be assumed that the crystallites belonging to the "low-stress" crystallization portion reveal average crystallite sizes of only ≈ 10 nm perpendicular to the chain axes, while the respective dimensions are significantly higher (15–25 nm) for the transcrystalline material portion.

For the uniaxially drawn ($\lambda = 1.1$) sample 2, the type of texture and the crystallite sizes remain approximately unchanged in comparison to sample 1. But in the (020) pole figure of sample 2 the maximum of orientation at N is significantly broader in N–M-direction than for the undrawn film [cf. Fig. 4(b) and Table I]. This finding shows a good correlation to TEM results (cf. also Ref. 26 for further details), for lamellar stacks of the same material with crystalline c-axes oriented in the M-direction. The visible stacks of lamellae have their growth directions (crystalline b-axes) preferentially oriented along N, i.e., the TEM micrographs (cf. Fig. 8) exhibits a characteristic proportion of the transcrystalline lamellae.

Although the micrograph of sample 1 [cf. Fig. 8(a)] indicates a random distribution of the length of lamellae (b-axes) with some larger lamellae preferentially oriented with their b-axes in the N-direction, the micrograph of sample 3 [cf. Fig. 8(c)] reveals a tendency of lamellae breaking combined with a slight change of orientation of b-axes towards M.

The crystallite size parameter $L_{020,\,N} = 11.8$ nm of sample 2, which is slightly but significantly decreased as compared with sample 1, also indicates that, even for relatively small drawing stresses, some crystallites of the transcrystalline proportion will break to smaller parts.

In the case of samples 3 ($\lambda = 5.0$) and 4 ($\lambda = 7.5$) the uniaxial drawing results in a completely new texture [cf. Figs. 5, 6, and 3(a)]. Now the a-, b-, and c-axes show orientation maxima in N-, T-, and M-directions, respectively (c-texture). An orientation maximum of crystalline b-axes along N is not visible for samples 3 and 4. The orientation maxima are much sharper than for samples 1 and 2.

Concerning the (002)-pole figures, it should be mentioned that there is an additional relative maximum of intensity in the normal direction N of the film. This intensity is supposed to result mainly from the overlap between the meridional (002) and the equatorial (520) reflection. The states of orientation recognized for samples 3 and 4 may be explained using the model of high stress crystallization under extremely high deformation stresses. (Note that there were solid films stretched during the drawing treatment.) The high stresses acting on samples 3 and 4 during drawing probably cause a rotation of the low stress crystallites present in the case of the starting material sample 1 around their fixed b-axes, in such a manner that after drawing the a-axes will be directed in N and the c-axes will show their orientation maximum in the drawing direction M.

The crystallites of the transcrystalline portion of sample 1, however, seem to vanish under high drawing stresses in the M-direction. This assumption is not only confirmed by the absence of the b-axes orientation maximum at N, but it is also hard to understand that a uniaxial drawing stress in the M-direction could cause a rotation of the b-axes of the transcrystalline proportion from the N-direction to T-direction. Furthermore, for the drawing product sample 4 only crystallite size parameters typical for the stress crystallization portion of sample 1 were found, but not the relatively high values of the transcrystalline material (cf. Table I). Intermediate crystallite size parameters were not found either.

The fact that the lateral crystallite sizes of sample 4 on average seem to be smaller than the lateral crystallite sizes of the stress crystallization portion of

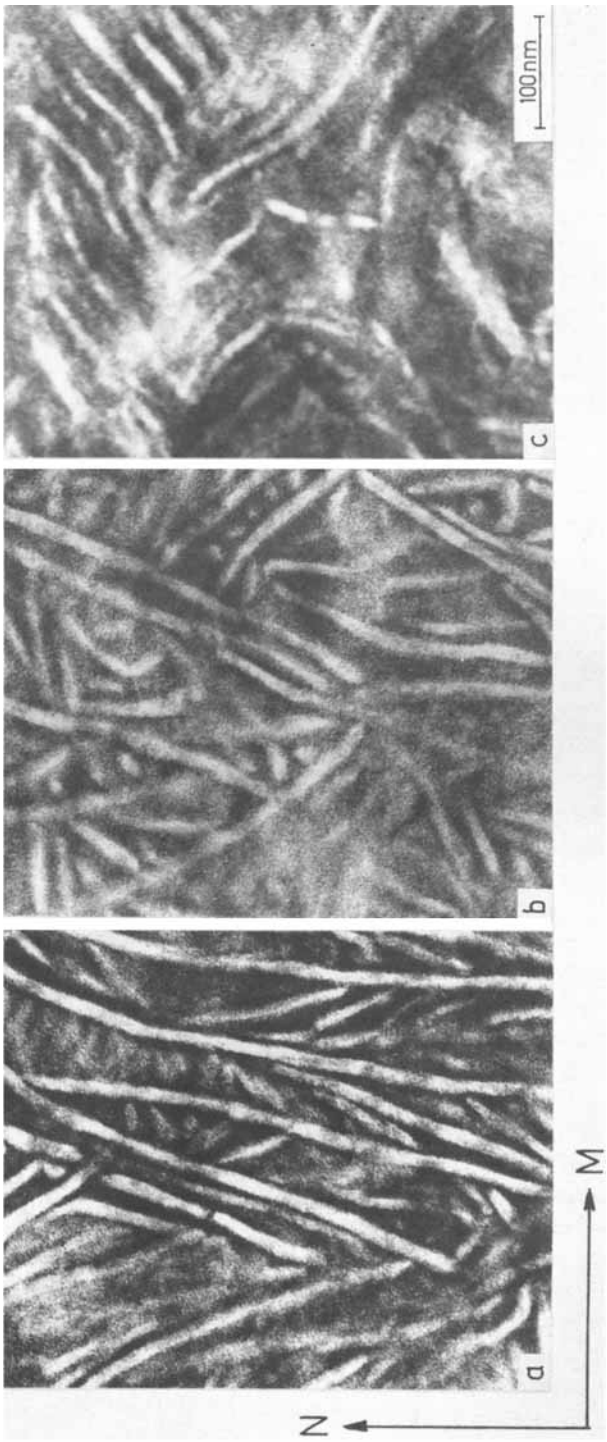

Fig. 8. TEM micrographs, direction of view parallel to T, i.e. at the MN plane (a) sample 1; (b) sample 2; (c) sample 3 (selectively stained specimens).

TABLE II
Quantitative Results of the Mechanical Investigations[a]

Parameter	Sample 1	Sample 2	Sample 3	Sample 4
E_M (MPa)	430	420	1320	1340
E_T (MPa)	560	560	840	902
σ_M (MPa)	35	51	52	113
σ_T (MPa)	27	25	23	21
ϵ_M (%)	1194	704	728	182
ϵ_T (%)	961	965	1088	952

[a] E_M = nearly statistically measured Young's modulus in the M direction. E_T = nearly statistically measured Young's modulus in the T-direction. σ_M = tensile strength in the M-direction. σ_T = tensile strength in the T direction. ϵ_M = elongation at break in the M-direction. ϵ_T = elongation at break in the T-direction.

the starting product sample 1 may be associated with a slight superposition of the orientation maxima of the stress crystallization material with the WAXS of a small amount of the transcrystalline proportion of sample 1, while sample 4 does not contain any considerable amount of transcrystalline material.

Although only the connections between structure and development and samples texture have been discussed as yet, we shall now briefly treat the correlations between some significant mechanical properties and the texture of samples 1–4. Young's moduli E_M and E_T, tensile strength values σ_M and σ_T, and the elongations at break, ϵ_M and ϵ_T, in the M- and T- directions of the films are documented in Table II. According to the literature cited above, a qualitative correlation is expected to exist between c-axes orientation and the anisotropy of the mechanical parameters just mentioned. For samples 1 and 2 a very broad orientation distribution of c-axes can be concluded from the (011) pole figures [cf. Fig. 4(a)]. This can easily be connected with the very similar E_M and E_T values and ϵ_M and ϵ_T values for both samples 1 and 2 and with the accordance of σ_M with σ_T for sample 1. The significant increase in the σ_M/σ_T ratio in the case of sample 2, however, cannot be directly explained by the c-axes orientation distribution.

For the higher drawn samples 3 and 4 together with the improved orientation of c-axes in the M-direction, an increase in the E_M/E_T, the σ_M/σ_T, and ϵ_T/ϵ_M ratios is to be established. This increase is especially pronounced for the tensile strength ratio of sample 4.

From the discussion we have had so far, it may be concluded that the state of orientation of blown LDPE films, which had been investigated by us earlier,[16] is also determined by a superposition of texture of differently crystallized material portions. The texture of the films produced at a low take-off velocity (V_A = 14 m/min) was similar to that in the case of HDPE samples 1 and 2 of our recent publication. Therefore the slow take-off samples of our former publication should also consist of a transcrystalline and a low stress crystalline material proportion. For the fast take off sample (V_A = 40 m/min), however, the axial deformation stress will result in a rotation of the crystallites around their b-axes, which remain in the T-direction. After drawing, the a-axes are mainly oriented in the N–M-plane with a maximum at an angle of $\sim 40°$ from M. On the other hand, the transcrystallization-depen-

dent partial texture seems to remain unchanged. [Note: As in the case of samples 1 and 2 the absence of a distinct orientation maximum in the T-direction of the (020)-pole figure of our earlier samples may be connected with the relatively broad distribution in the N–T-direction of the transcrystalline b-axes orientation maximum in N]. This explanation of the texture of the fast take-off sample may also be valid for the σ_{11}/σ_{22} = 4:1 sample of Choi et al.[15]

SUMMARY

It is to be established that blown PE films are an instructive example of the interconnections between different structure development mechanisms in crystallizing polymers. The results discussed demonstrate how important it is to combine different appropriate methods of structure investigation (i.e., X-ray scattering and EM investigations) if rather complex structure development processes in polymer crystallization are concerned.

For sample 1, which was blown under very low stresses ($\lambda \approx 1$, $\beta \approx 1$), and for the only slightly redrawn ($\lambda = 1.1$) sample 2, the parallel existence of very low stress crystalline and transcrystalline material portions was proved. The crystallites of the low stress portion are preferentially oriented with their a-axes in the M-direction (a-texture) and their lateral crystallite sizes are only half as great ($\approx$ 10 nm) as the respective quantities for the transcrystallites. The experimentally determined state of orientation is equivalent to the superposition of the individual textures of the two differently crystallized material portions.

The higher uniaxially drawn samples 3 and 4, however, reveal a texture comparable to that in the case of very high stress crystallization. Here drawing results in a rotation of the stress crystallized crystallites with their a- and c-axes around their fixed b-axis in such a manner that, after drawing, the a-axes are preferentially oriented in N and the c-axes are mainly directed along the M-direction (c-texture). In addition to this, the higher drawing ratios (cf. samples 3 and 4) obviously cause the almost total vanishing of the transcrystalline material portion. With one exception a correlation could be established between c-axes orientation and Young's modulus and tensile strength ratios E_M/E_T and σ_M/σ_T, respectively.

References

1. P. H. Lindenmeyer and S. Lustig, *J. Appl. Polym. Sci.*, **9**, 227 (1965).
2. C. R. Desper, *J. Appl. Polym. Sci.*, **13**, 169 (1969).
3. W. F. Maddams and J. E. Preedy, *J. Appl. Polym. Sci.*, **22**, 2721 (1978).
4. D. R. Holmes, R. G. Miller, R. P. Palmer, and C. W. Bunn, *Nature*, **171**, 1104 (1953).
5. D. R. Holmes and R. P. Palmer, *J. Polym. Sci.*, **31**, 345 (1958).
6. A. Keller, *J. Polym. Sci.*, **15**, 31 (1955).
7. S. L. Aggarwal, G. P. Tilley, and O. J. Sweeting, *J. Appl. Polym. Sci.*, **1**, 91 (1959).
8. C. R. Desper and R. S. Stein, *J. Appl. Phys.*, **37**, 3990 (1966).
9. W. F. Maddams and J. E. Preedy, *J. Appl. Polym. Sci.*, **22**, 2739 (1978).
10. W. F. Maddams and J. E. Preedy, *J. Appl. Polym. Sci.*, **22**, 2751 (1978).
11. W. F. Maddams and J. E. Preedy, *J. Appl. Polym. Sci.*, **22**, 3027 (1978).
12. T. Matsumata and T. Nagasawa, *Kobunshi Ronbunshu*, **33**, 171 (1976).
13. Y. Shimomura, J. E. Spruiell, and J. L. White, *Polym. Eng. Rev.*, **2**, 417 (1983).
14. M. Gilbert, D. A. Hemsley, and S. R. Patel, *Br. Polym. J.*, **19**, 9 (1987).

15. K. J. Choi, J. E. Spruiell, and J. L. White, *J. Polym. Sci. Polym. Phys. Ed.*, **20**, 27 (1982).
16. E. Walenta, A. Janke, D. Hofmann, D. Fanter, and D. Geiss, *Acta Polym.* **37**, 557 (1986).
17. D. Geiss and D. Hofmann, *Progr. Polym. Sci.*, to appear.
18. D. T. Keating, *Rev. Sci. Instrum.*, **30**, 725 (1959).
19. H. M. Heuvel, R. Huisman, and K. C. J. B. Lind, *J. Polym. Sci. Polym. Phys. Ed.*, **14**, 921 (1976).
20. H.-P. Fink, D. Fanter, and B. Philipp, *Acta Polym.*, **36**, 1 (1985).
21. A. Keller and M. J. Machin, *J. Macromol. Sci. Phys.*, **B1**, 41 (1967).
22. A. Keller and M. J. Hill, *J. Macromol. Sci. Phys.*, **B3**, 153 (1969).
23. R. K. Eby, *J. Appl. Phys.*, **35**, 2720 (1964).
24. D. Fitchmun and S. Newman, *J. Polym. Sci.*, **B7**, 301 (1969).
25. L. W. Bunn, *Trans. Faraday Soc.*, **35**, 482 (1939).
26. G. H. Michler, et al., in preparation.

Received June 30, 1989
Accepted July 18, 1989